JOURNAL OF AGRICULTURAL AND FOOD CHEMISTRY

Spreading of Monoglycerides onto β-Casein Adsorbed Film. Structural and Dilatational Characteristics

JUAN M. RODRÍGUEZ PATINO,* MARTA CEJUDO FERNÁNDEZ, M. ROSARIO RODRÍGUEZ NIÑO, AND CECILIO CARRERA SÁNCHEZ

Departamento de Ingeniería Química, Facultad de Química, Universidad de Sevilla, C/. Prof. García González 1, 41012 Seville, Spain

The effect of monoglycerides (monopalmitin and monoolein) on the structural, topographical, and dilatational characteristics of β-casein adsorbed film at the air−water interface has been analyzed by means of surface pressure (π)−area (*A*) isotherms, Brewster angle microscopy (BAM), and surface dilatational rheology. The static and dynamic characteristics of the mixed films depend on the interfacial composition and the surface pressure. At surface pressures lower than that for the β-casein collapse (at the equilibrium surface pressure of the protein, $\pi_e^{\beta-\text{casein}}$) a mixed film of β-casein and monoglyceride may exist. At higher surface pressures the collapsed β-casein is partially displaced from the interface by monoglycerides. However, β-casein displacement by monoglycerides is not quantitative at the monoglyceride concentrations studied in this work. The protein displacement by a monoglyceride is higher for monopalmitin than for monoolein and for spread than for adsorbed films. The viscoelastic characteristics of the mixed films were dominated by the presence of β-casein in the mixture. Even at the higher surface pressures (at $\pi > \pi_e^{\beta-\text{casein}}$) the small amounts of β-casein collapsed residues at the interface have a significant effect on the surface dilatational properties of the mixed films. The structural, topographical, and viscoelastic characteristics of the mixed films corroborate the fact that protein displacement for monoglycerides is higher for spread than for adsorbed mixed films.

KEYWORDS: Milk protein; β-casein; monoglyceride; monopalmitin; monoolein; air−water interface; adsorbed monolayer; spread monolayer; mixed monolayer; surface rheology

INTRODUCTION

Competitive adsorption and/or displacement between low molecular weight surfactants (LMWE: mono- and diglycerides, phospholipids, etc.) and proteins at fluid−fluid interfaces play a role in the formation and stability of food dispersions (emulsions and foams) (*1*−*7*). From a fundamental point of view, interactions, orientation phenomena, and domain structure are of particular interest (*3*, *5*, *7*−*9*). The emulsifier film structure is important from a practical point of view because it defines its emulsifying and foaming properties. In addition, the development of intermolecular associations between film-forming components at fluid interfaces leads to alterations in surface properties that have measurable rheological consequences (*10*, *11*). Moreover, interfacial rheology is a very sensitive technique for assessing structure and interactions between film-forming components (*10*, *11*). On the other hand, the dynamic behavior of emulsifier films is recognized as being of importance in the formation and stability of food colloids (*12*−*16*). The study of such dynamic behavior can be described by interfacial rheology. Interfacial rheology can be defined for both compressional deformation (dilatational rheology) and shearing motion of the interface (shear rheology). Dilatational rheology plays an important role in short-term stability during formation of food dispersions (*13*−*16*).

The aim of this work was to analyze the effect of monoglycerides (monopalmitin and monoolein) on the interfacial behavior of a model milk protein (β-casein) previously adsorbed at the air−water interface. We will consider emulsifier (protein, monoglycerides, and their mixtures) adsorption, interactions, structure, and topography at the interface and surface dilatational characteristics, as related to the formation and stability of food dispersions (emulsions and foams). Although the monolayer technique has been used successfully for studying the properties of mixed emulsifiers spread at the air−water interface (*8*), adsorbed films of mixed emulsifiers are more interesting from a technological point of view. However, there exists little information about these systems so far (*17*, *18*). In the last section of this paper the structural and dilatational characteristics of β-casein and β-casein−monoglyceride mixed films formed by adsorption or spreading of the protein will be compared. The comparison between adsorbed and spread films is of interest because the thermodynamic characteristics of spread films can be derived directly from experiments in a film balance, but is

* To whom correspondence should be addressed. Tel.: +34 95 4556446. Fax: +34 95 4556447. E-mail: jmrodri@us.es.

10.1021/jf053142r CCC: $33.50
Published on Web 04/21/2006

not possible for adsorbed films. Thus, the analysis of spread films may give additional insight for further study of adsorbed films. This paper complements previous works on pure proteins (*19*, *20*) and protein−monoglyceride mixed films adsorbed and spread at the air−water interface (*17*, *18*).

EXPERIMENTAL PROCEDURES

Chemicals. Synthetic 1-monohexadecanoyl-*rac*-glycerol (monopalmitin, DIMODAN^R PA 90) and 1-mono(*cis*-9-octadecanoyl) glycerol (monoolein, RYLO MG 19) were supplied by Danisco Ingredients (Brabran, Denmark) with over 95−98% purity. β-Casein (>99%) was supplied and purified from bulk milk from the Hannah Research Institute (Ayr, Scotland). Samples for interfacial characteristics of β-casein adsorbed films were prepared using Milli-Q ultrapure water and were buffered at pH 7. To form the mixed surface film on a previously adsorbed β-casein film, monoglyceride was spread in the form of a solution, using hexane:ethanol (9:1, v:v) as a spreading solvent. Analytical grade hexane (Merck, 99%) and ethanol (Merck, >99.8%) were used. The water used as subphase was purified by means of a Millipore filtration device (Milli-Q). A commercial buffer solution called trizma ($(CH_2OH)_3CNH_2/(CH_2OH)_3CNH_3Cl$, Sigma, >99.5%) was used to achieve pH 7. Ionic strength was 0.05 M in all the experiments.

Surface Film Balance. Measurements of surface pressure (π)−area (A) isotherms of adsorbed β-casein films and β-casein−monoglyceride mixed films at the air−water interface were performed on a fully automated Wilhelmy-type film balance (KSV 3000, Finland) as described previously (*10*, *11*). The maximum area of the trough between the two barriers is 51.5 × 15 cm^2. Before each measurement, the film balance was calibrated at 20 °C. For β-casein adsorbed films from water a protein solution at 1×10^{-5} wt % was left in the trough and time allowed for protein adsorption at the interface. This protein concentration was selected from previous data of the adsorption isotherm (*21*). At this protein concentration in solution the surface pressure after 24 h at the maximum area of the trough was practically zero. At this point the monoglyceride (monopalmitin or monoolein) was spread at different points on the β-casein film. Further details about operational conditions have been described elsewhere (*17*, *18*). Mixtures of particular mass fractions—expressed as the mass fraction of monopalmitin, X_{MP}, or monoolein, X_{MO}, in the mixture—were studied. The compression rate was 3.3 cm·min^{-1}, which is the highest value for which isotherms were found to be reproducible in preliminary experiments. The $\pi-A$ isotherm was measured four times. The reproducibility of the results was better than ±0.5 mN/m for surface pressure and ±0.05 m^2/mg for area.

Brewster Angle Microscopy (BAM). A commercial Brewster angle microscope (BAM), BAM2, manufactured by NFT (Göttingen, Germany) was used to study the topography of the film. The BAM was positioned over the film balance. Further characteristics of the device and operational conditions have been described elsewhere (*22*, *23*). The imaging conditions were adjusted to optimize image quality.

Surface Dilatational Rheology. To obtain surface rheological parameters—such as surface dilatational modulus (E), elastic (Ed) and viscous (Ev) components, and loss angle tangent (Tan θ)—the same modified Wilhelmy-type film balance (KSV 3000) was used as described elsewhere (*10*, *11*). In this method the surface is subjected to small periodic sinusoidal compressions and expansions by means of two oscillating barriers at a given frequency (ω) and amplitude ($\Delta A/A$) and the response of the surface pressure is monitored. Surface pressure was directly measured by means of two roughened platinum plates situated on the surface between the two barriers. The dilatational modulus is a complex quantity and is composed of real and imaginary parts (E = Ed + i Ev). The real part of the dilatational modulus or storage component is the dilatational elasticity, Ed = $|E|\cdot\cos\theta$. The imaginary part of the dilatational modulus or loss component is the surface dilatational viscosity, Ev = $|E|\cdot\sin\theta$. The loss angle tangent can be defined as the ratio between the viscous and elastic components of the modulus (Tan θ = Ev/Ed). If the film is purely elastic, the loss angle tangent is zero. The amplitude of deformation was maintained constant at 5%. This percentage area change was determined to be in the linear region. The reproducibility of these results for two measurements was better than 5%.

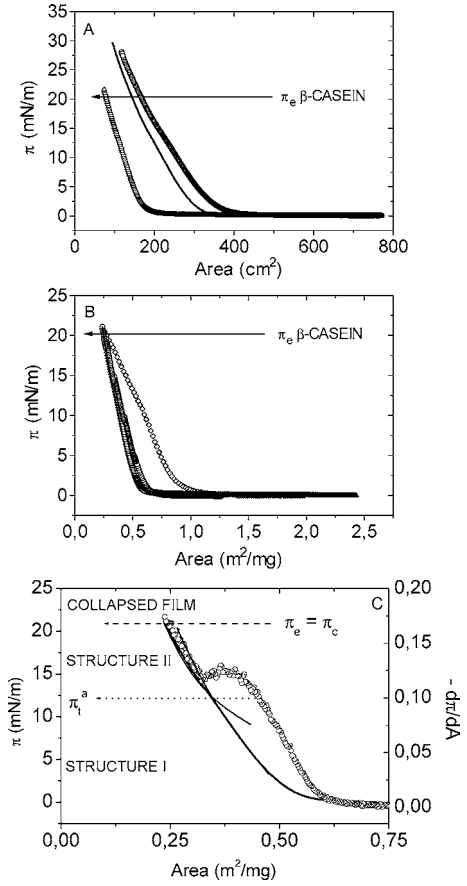

Figure 1. (**A**) π–trough area isotherms for an adsorbed film of β-casein after successive compressions, at (△) 9 h, (○) 23 h, and (—) 24 h. (**B**) $\pi-A$ isotherms for (○) adsorbed β-casein films at an aging time of (△) 9 h, (○) 23 h, and (—) 24 h (compression curve), and (◇) spread β-casein monolayer (compression curve) (*11*). (**C**) $\pi-A$ isotherm (—) and (○) compressional coefficient ($\kappa = -d\pi/dA$) for an adsorbed β-casein film at an aging time of 24 h (compression curve). The transition between structures I and II (π_t^a) deduced by (dotted arrow) the point of intersection of two lines drawn according to a virial equation (*37*) or by (solid arrow) the compressional coefficient according to the method applied by Rosenholm et al. (*38*) is indicated. The equilibrium surface pressure (π_e) and the collapse pressure (π_c) of β-casein adsorbed film are indicated by a dashed arrow. Aqueous subphase at pH 7. Temperature 20 °C. The π_e of β-casein is indicated by means of an arrow.

RESULTS AND DISCUSSION

Structural Characteristics of β-Casein Adsorbed Films. **Figure 1A** shows the π−trough area isotherms for an adsorbed film of β-casein after successive compressions, formed from adsorption in solution at 1×10^{-5} wt %. In these experiments π−trough area isotherms at different times after the spreading, starting at 30 min and lasting 48 h, have been recorded. However, to add clarity only three π−trough area isotherms are included in **Figure 1A**. There was a difference in the π−trough area isotherms as a function of time after protein addition to the aqueous bulk phase. It can be seen that there was a shift of the π−trough area isotherms toward higher areas as the protein adsorption time increased to 23 h. This phenomenon may be attributed to adsorption of β-casein at the interface, which increased with the adsorption time, and in a minor degree due to the unfolding of the protein, because β-casein is a

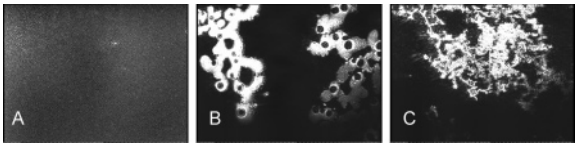

Figure 2. Visualization of β-casein films by Brewster angle microscopy at 20 °C. (**A**) This picture was observed for β-casein adsorbed films during the first film compression. The same image was observed for β-casein spread monolayers during the first compression and after successive compressions (*23*, *29*). (**B**) β-Casein aggregates in adsorbed films at the end of the first compression (at $\pi \geq 21$ mN/m). (**C**) β-Casein aggregates in adsorbed films at the end of the first expansion and at the beginning of successive compressions (at $\pi \geq 0$ mN/m). The same picture was observed in some spots at higher surface pressures. The horizontal direction of the image corresponds to 630 μm and the vertical direction to 470 μm.

disordered protein. In fact, the π−trough area isotherm for a first compression at 30 min of adsorption time indicates that a small amount of protein was adsorbed at the interface, although the surface pressure at the minimum area was the same as the equilibrium surface pressure for β-casein ($\pi_e \cong 20.9$ mN/m) (*21*). The maximum surface pressure also increased with the aging time. In addition, the π−trough area isotherms were parallel after successive compressions. These data reveal that a long time interval of adsorption allows more β-casein to adsorb at the surface, especially from low protein concentrations in solution such as those used in this work. After 23 h of adsorption time the π−trough area isotherms after repetitive compression−expansion cycles show a shift toward lower areas, which may be explained by a condensation of the protein at the interface.

Since the surface concentration is actually unknown for the adsorbed film, the values were derived by assuming (**Figure 1B**) that the area for adsorbed and spread films was equal at the collapse point (*17*, *19*, *24*). This assumption can be supported by the fact that, for β-casein films, the equilibrium spreading pressure (π_e) and the surface pressure at the plateau for a saturated β-casein adsorbed film (*21*) are the same.

The π−A isotherms deduced for adsorbed β-casein films in the Wilhelmy-type film balance are in good agreement with those observed in the Langmuir-type film balance (*18*). The results of the π−*A* isotherms with the help of the compressional coefficient (**Figure 1C**) deduced from the slope of the π−*A* isotherm ($\kappa = -d\pi/dA$), indicate that adsorbed β-casein films at the air−water interface adopt two different structures or condensation states and the collapse phase. At low surface pressures (at $\pi < 12$ mN/m) adsorbed β-casein films exist (*25*) as trains with amino acid segments located at the interface (structure I). At higher surface pressures (at $\pi > 12$ mN/m), and up to the equilibrium surface pressure, amino acid segments are extended into the underlying aqueous solution and adopt the form of loops and tails (structure II). The film collapses at a surface pressure ($\pi_e^{\beta-\text{casein}}$) of about 21 mN/m (**Figure 1B**), a value close to the surface pressure at the plateau for a saturated adsorbed film and to the equilibrium surface pressure (*21*).

BAM images prove that the morphology of adsorbed β-casein monolayers during the first compression is uniform (**Figure 2A**), suggesting homogeneity in thickness and film isotropy. However, interfacial regions with folds or aggregations of collapsed β-casein, which were formed at the higher surface pressures (**Figure 2B**), were observed at the interface during the monolayer expansion, even at the lowest surface pressure, at $\pi \approx 0$ mN/m (**Figure 2C**). These heterogeneities at a microscopic level were also observed at the interface after repetitive compressions of the monolayer. The reflectivity (data not shown) as a function

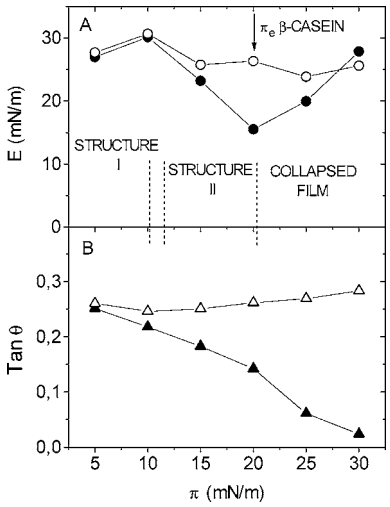

Figure 3. Surface pressure dependence of (**A**) surface dilatational modulus (*E*) and (**B**) loss angle tangent (Tan θ) for pure β-casein films at pH 7 and at 20 °C. Open symbols are for adsorbed films—concentration of β-casein in the aqueous phase 1×10^{-5} wt %—and closed symbols are for spread monolayers (*11*). The frequency (50 mHz) and amplitude (5%) of deformation were maintained constant. The π_e of β-casein is indicated by means of an arrow.

of surface pressure obtained with β-casein adsorbed films shows that film thickness increases with the surface pressure and is a maximum at the collapse, at the highest surface pressure.

Dilatational Characteristics of β-Casein Adsorbed Films. For β-casein adsorbed films the surface dilatational modulus (*E*) versus surface pressure plots showed an irregular shape (**Figure 3A**). The modulus (*E*) increased with increasing surface pressure to a maximum value at a surface pressure which corresponds to the π value of the transition between structures I and II. Upon further increase of the surface pressure *E* decreased to a minimum at a surface pressure of about 20 mN/m, close to the collapse point. Afterward, *E* values increased again with surface pressure. The increase of *E* at the higher π may be due to the formation of protein multilayers. The same irregular shape in the surface pressure dependence of the surface dilatational modulus was observed by other authors for β-casein adsorbed films (*15*, *16*), the values of *E* being of the same order as those in **Figure 3A**. These results are also essentially the same as those deduced from the slope of the π−*A* isotherm, with the minimum value of *E* at the collapse point (data not shown).

On the other hand, the points of inflection in the *E*−π curves coincide with the transition between structures I and II and between structure II and film collapse, respectively. That is, the interactions between amino acid residues in β-casein adsorbed films with a tail conformation (structure I) are stronger than those between amino acid residues with tail and loop conformations (structure II). Finally, the evolution of Tan θ with π (**Figure 3B**) corroborates that adsorbed β-casein films present viscoelastic behavior at every surface pressure. These results confirm that surface dilatational rheology is sensitive to the structure and interactions in β-casein adsorbed films at the air−water interface.

Changes in surface dilatational properties (*E* and Tan θ) for β-casein adsorbed films, as a function of frequency of oscillation over a range of 50−200 mHz, at two surface pressures (at 20 mN/m and at the collapse point), are illustrated in **Figure 4**. It can be seen that (i) the *E* values for adsorbed β-casein films are practically constant and (ii) Tan θ values increase with the

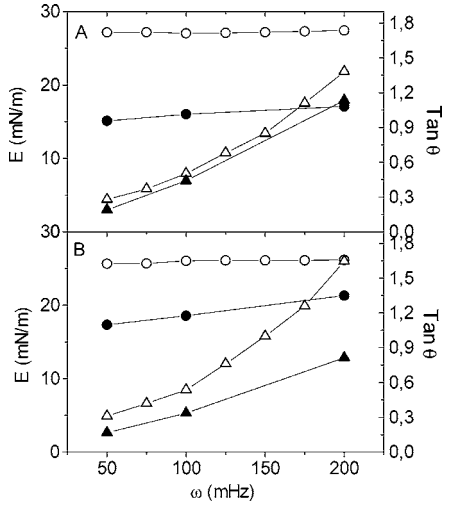

Figure 4. Frequency dependence of surface dilatational modulus (*E*) and loss angle tangent (Tan θ) for pure β-casein films at (**A**) 20 mN/m and (**B**) at the collapse point. Temperature 20 °C and pH 7. Symbols: (○, ●) surface dilatational modulus at 20 mN/m and (△, ▲) loss angle tangent. Open symbols are for adsorbed films—concentration of β-casein in the aqueous phase 1×10^{-5} wt %—and closed symbols are for spread monolayers (*11*). Amplitude of deformation: 5%.

frequency for adsorbed β-casein films. These results are in good agreement with those obtained for β-lactoglobulin (*12*, *26*), β-casein (*27*), and BSA (*27*, *28*) adsorbed films. From the effect of frequency on surface dilatational parameters it can be concluded that adsorbed β-casein films present rheological behavior in dilatational conditions that is viscoelastic within the range of frequencies studied. As a consequence of the viscoelastic behavior, the loss tangent angle increases with frequency. The frequency dependence of surface dilatational properties may be associated with the effect of the rate of deformation on the structure of β-casein films. The viscoelastic behavior observed for β-casein adsorbed films may be associated with the exchange of protein residues in the form of tails and/or loops within the interface (*11*, *12*, *15*, *16*, *26*) and/or with the organization/reorganization of film structure (*11*) at 20 mN/m (**Figure 4A**) and with the formation/destruction of 3-D collapse structures (including multilayer formation) at the collapse point (**Figure 4B**).

Structural, Topographical, and Dilatational Characteristics of β-Casein−Monopalmitin Mixed Films Adsorbed at the Air−Water Interface. Mixtures of particular β-casein/monopalmitin mass fraction expressed as the mass fraction of monopalmitin in the mixture (at X_{MP} of 0, 0.25, 0.4, and 1.0) were studied. The amount of spread monoglyceride was calculated on the basis of the mass of previously adsorbed β-casein (which was deduced from the adsorbed $\pi-A$ isotherm). Thus, as opposed to spread monolayers (*29*), for adsorbed films the mixtures with mass fractions higher than $X_{MP} = 0.4$ saturate the interface under the experimental conditions used in this work.

The surface pressure as a function of the trough area for β-casein + monopalmitin adsorbed mixed films (compression curves) is shown in **Figure 5A**. As for pure β-casein adsorbed films, the actual $\pi-A$ isotherms for β-casein + monopalmitin adsorbed mixed films were derived by assuming (*17*, *18*) that the *A* value for adsorbed and spread films was equal at the collapse point. This assumption can be supported by the fact that the surface pressure at the collapse point for adsorbed (**Figure 5B**) and spread (*29*) mixed films is practically equal

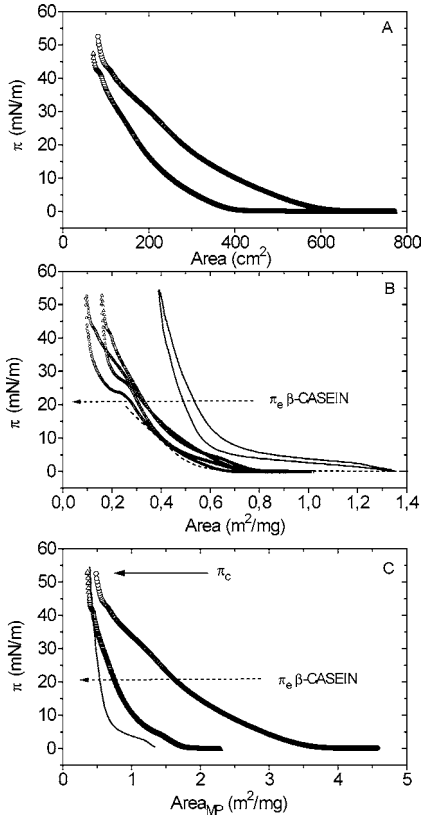

Figure 5. (**A**) Surface pressure–trough area isotherms (compression curves) and (**B**) surface pressure–area isotherms (compression–expansion curves) for pure components and mixed films of monopalmitin spread on a β-casein adsorbed film from buffered water at pH 7 and at 20 °C. (C) Surface pressure–area isotherms (compression curves) for mixed films of monopalmitin spread on a β-casein adsorbed film on the basis that only monopalmitin is present at the air–water interface. Concentration of β-casein in the aqueous phase 1×10^{-5} wt %. Mass fraction of monopalmitin in the mixture: (---) 0, (○) 0.25, (△) 0.40, and (—) 1.0. The collapse point (π_c) of the mixed films is indicated by a continuous arrow. The equilibrium surface pressure (π_e) of β-casein is indicated by means of a discontinuous arrow.

to that for the pure monoglyceride. Results derived from $\pi-A$ isotherms for β-casein + monoglyceride adsorbed mixed films with this assumption were the same (within the experimental deviations admitted in these experiments for surface pressure and area) as those deduced from the amount of spread monoglyceride calculated on the basis of the mass of previously adsorbed β-casein. These results (**Figure 5B**) are also in good agreement with those obtained in the Langmuir-type trough with the same β-casein + monopalmitin adsorbed mixed films (*18*).

Briefly, (i) there was a film expansion as the monopalmitin concentration in the mixture was increased, especially at higher surface pressures. That is, the $\pi-A$ isotherm is displaced toward higher *A* as the concentration of monopalmitin in the mixture increases. (ii) At surface pressures higher than that for β-casein collapse ($\pi_e^{\beta-\text{casein}}$), the $\pi-A$ isotherm for mixed films was parallel to that of monopalmitin. (iii) The hypothetical $\pi-A$ isotherms for β-casein + monopalmitin adsorbed mixed films, calculated on the basis that only monopalmitin is present at the air−water interface (**Figure 5C**), at $\pi > \pi_e^{\beta-\text{casein}}$, tend to that of a pure monopalmitin spread monolayer, especially at the higher π and X_{MP} in the mixture. These results suggest that at $\pi > \pi_e^{\beta-\text{casein}}$ protein displacement by the monoglyceride from the air−water interface takes place. At $\pi < \pi_e^{\beta-\text{casein}}$ both β-casein and monopalmitin coexist at the interface and the $\pi-A$

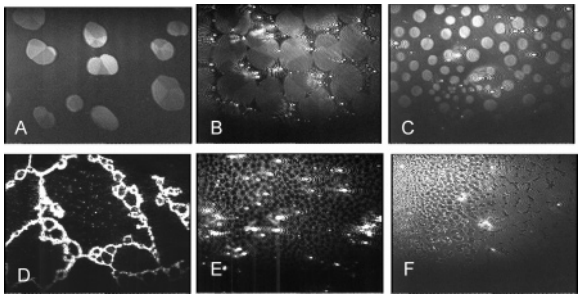

Figure 6. Visualization of β-casein–monopalmitin adsorbed mixed films by Brewster angle microscopy at 20 °C. (**A**) Monopalmitin at 10 mN/m. The same image was observed for β-casein–monopalmitin adsorbed mixed film at π < 18 mN/m. (**B**) Monopalmitin at 30 mN/m. (**C**) β-Casein + monopalmitin adsorbed film at 15 mN/m. (**D**) β-Casein + monopalmitin adsorbed film at π < 22 mN/m. (**E**) β-Casein + monopalmitin adsorbed film at 32 mN/m. (**F**) β-Casein + monopalmitin adsorbed film at 49 mN/m. The horizontal direction of the image corresponds to 630 μm and the vertical direction to 470 μm.

isotherms of adsorbed mixed films and a spread monopalmitin monolayer (i.e., the monolayer structures) are different (**Figure 5C**). At the highest surface pressures, at the collapse point of the mixed film, immiscibility between film-forming components is deduced due to the fact that the collapse pressure of mixed films is similar to that of a pure monoglyceride monolayer (**Figure 5B**). (iv) The protein displaced by monopalmitin from the interface during compression remains underneath the monoglyceride film either through hydrophobic interactions between protein and lipid or by local anchoring through the monoglyceride layer (*17*, *18*, *30*) and re-enters the mixed film during the expansion. This statement is supported by the fact that the $\pi-A$ isotherms were repetitive after continuous compression−expansion cycles (data not shown). (v) For adsorbed β-casein−monopalmitin mixed films a first-order-like phase transition was observed upon film expansion (**Figure 5B**) at surface pressures close to the equilibrium surface pressure of β-casein—with a degenerated plateau in the $\pi-A$ isotherm. This result suggests that the re-adsorption of previously displaced β-casein has kinetic character (*17*, *18*).

The evolution with the surface pressure of BAM images (**Figure 6**) gives complementary information, at a microscopic level, on the structural characteristics and interactions of adsorbed β-casein−monopalmitin mixed films, as deduced from $\pi-A$ isotherms (**Figure 5**). At $\pi < \pi_e^{\beta-\text{casein}}$ a mixed film of monopalmitin and β-casein may exist (**Figure 6C**) with small domains of monopalmitin uniformly distributed on the homogeneous β-casein layer. The same image is characteristic of a pure monopalmitin monolayer with a liquid condensed structure at π > 5 mN/m. The circular domains of liquid condensed monopalmitin in the mixed film were more numerous as the surface pressure increased, as for a pure monopalmitin monolayer (**Figure 6B**). At $\pi > \pi_e^{\beta-\text{casein}}$ a characteristic squeezing out phenomena of β-casein by monopalmitin was observed (**Figure 6E**) and the mixed films were practically dominated by monopalmitin molecules. That is, at higher surface pressures, collapsed β-casein residues (bright region) may be displaced from the interface by monopalmitin molecules (circular dark regions). A topographical characteristic of the adsorbed film was the presence of short fractures in the film at the higher surface pressures, near the collapse point of the mixed film (**Figure 6F**), which are characteristic of protein−monoglyceride adsorbed films (*17*, *18*). During repetitive compressions of the mixed film some spots with folds or aggregations of collapsed

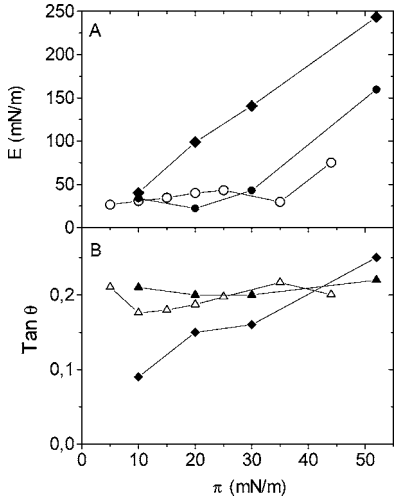

Figure 7. Surface pressure dependence of (**A**) surface dilatational modulus (*E*) and (**B**) loss angle tangent (Tan θ) for mixed films of monopalmitin and β-casein in buffered water at pH 7 and at 20 °C. Symbols: (○, △) mixed films of monopalmitin spread on a β-casein adsorbed film at a mass fraction of monopalmitin in the mixture of 0.25, (●, ▲) monopalmitin and β-casein spread mixed films at a mass fraction of monopalmitin in the mixture of 0.20 (*31*), and (◆) pure monopalmitin spread monolayer. Concentration of β-casein in the aqueous phase 1×10^{-5} wt %. Open symbols are for adsorbed films and closed symbols are for spread monolayers. The frequency (50 mHz) and amplitude (5%) of deformation were maintained constant.

β-casein, which were formed during the first compression of the film, were also observed (**Figure 6D**).

The surface viscoelastic properties of β-casein−monopalmitin adsorbed mixed films on the air−water interface at a representative monopalmitin concentration in the mixture of $X_{PM} = 0.25$ are shown in **Figure 7**. It can be seen that at $\pi < \pi_e^{\beta-\text{casein}}$ the $E-\pi$ plot showed an irregular shape (**Figure 7A**), as for a pure β-casein adsorbed film (**Figure 3A**). These results corroborate the idea that at $\pi < \pi_e^{\beta-\text{casein}}$ β-casein and monopalmitin coexist in adsorbed mixed films at the air−water interface. At $\pi > \pi_e^{\beta-\text{casein}}$ the value of *E* developed a maximum and then decreased to a minimum upon further increase of the surface pressure. At the higher surface pressures the $E-\pi$ plots for mixed films were parallel to those of monopalmitin, which demonstrated again that at higher surface pressures the mixed films were practically dominated by monopalmitin molecules. However, the data in **Figure 7A** also demonstrate that the small amounts of β-casein collapsed residues at the interface—as deduced at a microscopic level from BAM images (**Figure 6**)—have an effect on the surface dilatational properties of the mixed films. In fact, the values of *E* for mixed films are lower than those for a pure monopalmitin monolayer, even at the collapse point of the mixed films. Thus, the mechanical properties of the mixed films also demonstrated that, even at the highest surface pressure, a monopalmitin monolayer is unable to completely displace β-casein molecules from the air−water interface.

From the values of the loss angle tangent (Tan $\theta-\pi$ curves) for monopalmitin and β-casein−monopalmitin mixed films it can be concluded that these films behaved as viscoelastic at every surface pressure (**Figure 7B**). For the mixed films the values of Tan θ are the same no matter what the surface pressure. The results suggest that the presence of β-casein in the mixed film controls the viscoelasticity of the mixed films at $\pi < \pi_e^{\beta-\text{casein}}$ (at these surface pressures the values of Tan θ of the mixed films are similar to those of a pure β-casein

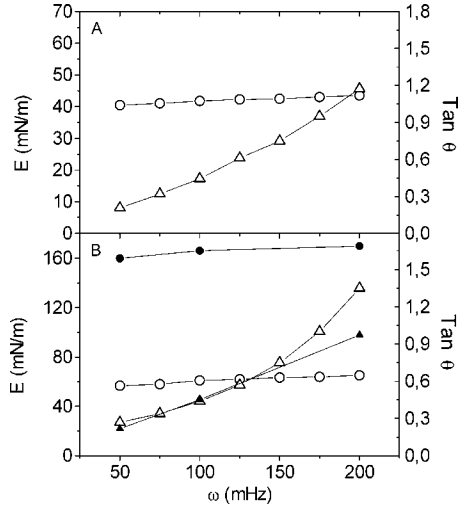

Figure 8. Frequency dependence of (○, ●) surface dilatational modulus (E) and (△, ▲) loss angle tangent (Tan θ) for mixed films of monopalmitin and β-casein at (**A**) 20 mN/m and (**B**) at the collapse point. Temperature 20 °C and pH 7. Symbols: (○, △) mixed films of monopalmitin spread on a β-casein adsorbed film at a mass fraction of monopalmitin in the mixture of 0.25—concentration of β-casein in the aqueous phase 1×10^{-5} wt %—and (●, ▲) monopalmitin and β-casein spread mixed films at a mass fraction of monopalmitin in the mixture of 0.20 (*31*). Amplitude of deformation: 5%.

adsorbed film), but this viscoelasticity is controlled by the presence of monopalmitin at the higher surface pressures (at $\pi > \pi_e^{\beta-\text{casein}}$ the values of Tan θ of the mixed films tend to those of a pure monopalmitin spread monolayer).

Changes in surface dilatational properties (E and Tan θ) with the frequency of oscillation for β-casein−monopalmitin adsorbed films at a representative mass fraction of monopalmitin in the mixture (at $X_{MP} = 0.25$) are illustrated in **Figure 8**. The frequency of oscillation over a range of 50−200 mHz and two surface pressures (at 20 mN/m and at the collapse point) are analyzed as variables. It can be seen that at $\pi = 20$ mN/m (**Figure 8A**) (i) the E values for adsorbed β-casein films are practically constant and (ii) the Tan θ values increase with the frequency. Thus, the same statements as those deduced for pure β-casein adsorbed films can be applied here. That is, the viscoelastic behavior is dominated by the presence of the protein in the mixed films. However, at the collapse point (**Figure 8B**), although the E and Tan θ values follow the same evolution with the frequency as for 20 mN/m, the E values are lower than that for a pure β-casein adsorbed film. Thus, it can be concluded that at $X_{MP} = 0.25$ monopalmitin is unable to displace a β-casein adsorbed film from the air−water interface, even at the highest surface pressure (at the collapse point of the mixed film).

Structural, Topographical, and Dilatational Characteristics of β-Casein−Monoolein Mixed Films Adsorbed at the Air−Water Interface. The structural characteristics of adsorbed β-casein−monoolein mixed films were essentially different from those of β-casein−monopalmitin, as deduced from $\pi-A$ isotherms (**Figure 9**). Briefly, as expected (*18*, *29*), β-casein−monoolein mixed films (**Figure 9B**) at surface pressures lower than that for β-casein collapse ($\pi_c^{\beta-\text{casein}} \cong 21$ mN/m) adopt a liquidlike-expanded structure, as for pure components. There was a film expansion due to the presence of monoolein in the mixture. At $\pi > \pi_e^{\beta-\text{casein}}$ the $\pi-A$ isotherms for mixed films were practically parallel to those of monoolein. At these experimental conditions the hypothetical $\pi-A$ isotherms for mixed films calculated on the basis that only monoolein is

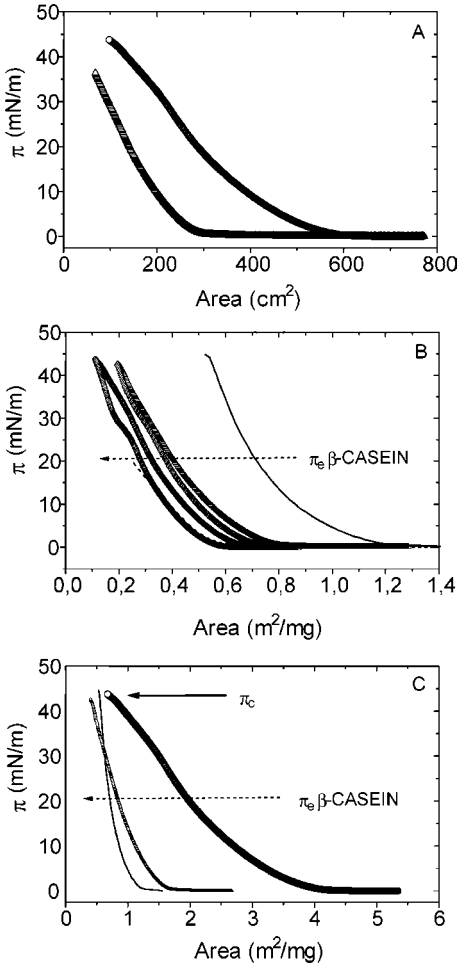

Figure 9. (**A**) Surface pressure–trough area isotherms (compression curves) and (**B**) surface pressure–area isotherms (compression–expansion curves) for pure components and mixed films of monoolein spread on β-casein adsorbed films from buffered water at pH 7 and at 20 °C. (**C**) Surface pressure–area isotherms (compression curves) for mixed films of monoolein spread on a β-casein adsorbed film on the basis that only monoolein is present at the air–water interface. Concentration of β-casein in the aqueous phase 1×10^{-5} wt %. Mass fraction of monoolein in the mixture: (---) 0, (○) 0.20, (△) 0.35, and (—) 1.0. The collapse point (π_c) of the mixed films is indicated by a continuous arrow. The equilibrium surface pressure (π_e) of β-casein is indicated by means of a discontinuous arrow.

present at the air−water interface tend to that of a pure monoolein monolayer (**Figure 9C**). These results prove that β-casein is partially displaced from the air−water interface by monoolein. At the highest surface pressures, at the collapse point of the mixed film, immiscibility between film-forming components is deduced due to the fact that the collapse pressure of mixed films is similar to that of a pure monoolein monolayer (**Figure 9B**). Interestingly, the re-adsorption of previously displaced β-casein upon the expansion is easier for monoolein than for monopalmitin because the hysteresis in the $\pi-A$ isotherms during the compression−expansion cycle is lower for β-casein-monoolein (**Figure 9B**) than for β-casein adsorbed monopalmitin (**Figure 5B**) films.

BAM images for adsorbed β-casein−monoolein mixed films were also different from those described above for adsorbed β-casein−monopalmitin mixed films (**Figure 10**). At $\pi < \pi_e^{\beta-\text{casein}}$ the topography of pure components and the mixed film is practically identical because in this region both components and the mixed film form an isotropic (homogeneous) film

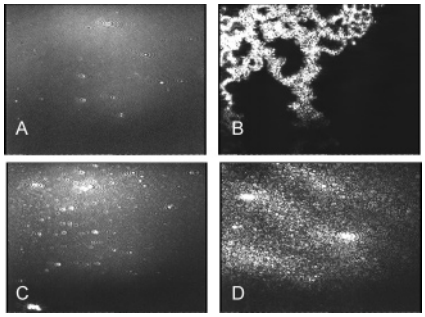

Figure 10. Visualization of β-casein–monoolein mixed films by Brewster angle microscopy at 20 °C. (**A**) This picture was observed for β-casein adsorbed films during the first film compression. The same image was observed for β-casein–monoolein mixed films at $\pi < \pi_e^{\beta-\text{casein}}$. (**B**) β-Casein aggregates in adsorbed β-casein–monoolein mixed films at 14–17 mN/m. (**C**) β-Casein + monoolein adsorbed film at 29 mN/m. (**D**) β-Casein + monoolein adsorbed film at 29–44 mN/m. The horizontal direction of the image corresponds to 630 μm and the vertical direction to 470 μm.

without any difference in the domain topography (**Figure 10A**). During repetitive compressions of the mixed film some spots with folds or aggregations of collapsed β-casein, which were formed during the first compression of the film, were also observed (**Figure 10B**). At surface pressures near to and after β-casein collapse BAM images (**Figure 10C**) demonstrated that monoolein and β-casein molecules adopted an isotropic structure in the mixed film with some white regions, which correspond to the presence of a thicker β-casein collapsed film. At the higher surface pressures, and especially at the collapse point, the topography of the mixed film was dominated by the presence of small domains of collapsed β-casein and monoolein at the interface (**Figure 10D**).

The surface viscoelastic properties of β-casein−monoolein adsorbed mixed films on the air−water interface at a representative monoolein concentration in the mixture of $X_{PM} = 0.25$ are shown in **Figure 11**. It can be seen that at $\pi < \pi_e^{\beta-\text{casein}}$ the $E-\pi$ plot showed (**Figure 11A**) the same evolution as for β-casein−monopalmitin adsorbed mixed films (**Figure 7A**). In addition, the E values for the adsorbed mixed films were the same no matter which monoglyceride is present in the mixture (either monopalmitin or monoolein), the $E-\pi$ plot showing an irregular shape, as for a pure β-casein adsorbed or spread films (**Figure 3A**). Thus, the differences between E values for a pure monoglyceride monolayer and adsorbed mixed films are higher for β-casein−monopalmitin (**Figure 7A**) than for β-casein−monoolein (**Figure 11A**) mixed films because the E values are higher for monopalmitin than for monoolein spread monolayers. These differences reach a maximum at the highest surface pressure, at the collapse point of the mixed films. Finally, at $\pi > \pi_e^{\beta-\text{casein}}$ the $E-\pi$ plots for mixed films were not parallel to those of monoolein (**Figure 11A**) as observed for β-casein−monopalmitin adsorbed mixed films (**Figure 7A**). These results demonstrate that the presence of β-casein in the mixture has an effect on E values of the mixed films, even at higher surface pressures ($\pi > \pi_e^{\beta-\text{casein}}$).

From the values of the loss angle tangent (Tan $\theta-\pi$ curves) for monoolein and β-casein−monoolein adsorbed mixed films it can be concluded that these films behaved as viscoelastic at every surface pressure (**Figure 11B**). For the mixed films the values of Tan θ are the same no matter what the surface pressure. The results suggest that the presence of β-casein in the mixed film controls the viscoelasticity of the mixed films

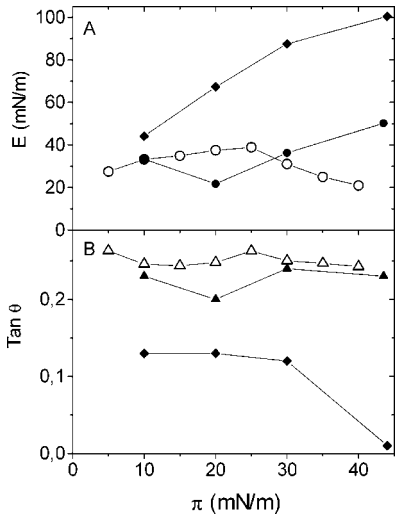

Figure 11. Surface pressure dependence of (**A**) surface dilatational modulus (E) and (**B**) loss angle tangent (Tan θ) for mixed films of monoolein and β-casein in buffered water at pH 7 and at 20 °C. Symbols: (○, △) mixed films of monoolein spread on a β-casein adsorbed film at a mass fraction of monoolein in the mixture of 0.25, (●, ▲) monoolein and β-casein spread mixed films at a mass fraction of monoolein in the mixture of 0.20 (*31*), and (♦) pure monoolein spread monolayer. Concentration of β-casein in the aqueous phase 1×10^{-5} wt %. The frequency (50 mHz) and amplitude (5%) of deformation were maintained constant. Open symbols are for adsorbed films and closed symbols are for spread monolayers.

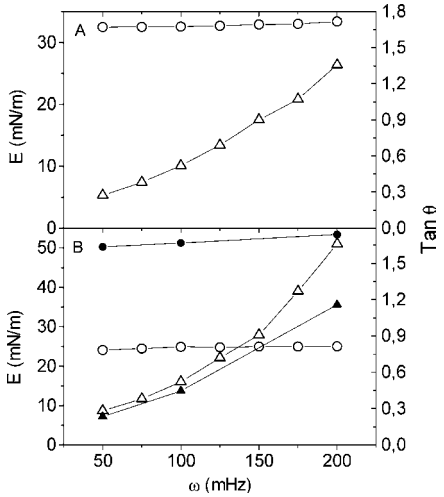

Figure 12. Frequency dependence of (○, ●) surface dilatational modulus (E) and (△, ▲) loss angle tangent (Tan θ) for mixed films of monoolein and β-casein in buffered water at (**A**) 20 mN/m and (**B**) at the collapse point. Temperature 20 °C and pH 7. Symbols: (○, △) mixed films of monoolein spread on a β-casein adsorbed film at a mass fraction of monoolein in the mixture of 0.25— concentration of β-casein in the aqueous phase 1×10^{-5} wt %—and (●, ▲) monoolein and β-casein spread mixed films at a mass fraction of monoolein in the mixture of 0.20 (*31*). Amplitude of deformation: 5%.

at every π (at these surface pressures the values of Tan θ of the mixed films are similar to those of a pure β-casein adsorbed film).

Changes in surface dilatational properties (E and Tan θ) with the frequency of oscillation for β-casein−monoolein adsorbed films at a representative mass fraction of monopalmitin in the mixture (at $X_{MP} = 0.25$) are illustrated in **Figure 12**. The frequency of oscillation over a range of 50−200 mHz and two

surface pressures (at 20 mN/m and at the collapse point) are analyzed as variables. From these results the same statements as those deduced for β-casein−monopalmitin adsorbed mixed films (**Figure 8**) can be applied. Thus, it can be concluded that at $X_{MO} = 0.25$ monoolein is unable to displace a β-casein adsorbed film from the air−water interface, even at the highest surface pressure (at the collapse point of the mixed film).

The viscoelastic characteristics of β-casein−monoglyceride mixed films can explain the differences observed during the re-adsorption (penetration) of displaced β-casein upon the expansion of a film previously compressed up to the collapse point (**Figures 5B** and **9B**). In fact, the re-adsorption (penetration) of previously displaced β-casein upon the expansion is easier for monoolein (**Figure 9B**) than for monopalmitin (**Figure 5B**) because β-casein−monopalmitin (**Figure 7A**) forms a much more elastic surface than β-casein−monoolein (**Figure 11A**) mixed film. The presence of the viscoelastic β-casein−monopalmitin mixed film (**Figure 7A**) prevents the penetration of previously displaced β-casein, upon the expansion of the film. These results support the hypothesis that as the interactions between film-forming components are stronger, which form a more elastic interface, the interface penetration is reduced (*7*). That is, the key features controlling the displacement or penetration of proteins into a fluid interface are the strength and elasticity of the film (*32*).

Comparison of Structural and Dilatational Characteristics of β-Casein and β-Casein−Monoglyceride Mixed Films Formed by Adsorption or Spreading of the Protein. *Adsorbed and Spread β-Casein Films.* The π−*A* isotherm deduced for adsorbed β-casein films is more condensed than that obtained directly by spreading (**Figure 1B**). One possibility is that the slow formation of the adsorbed film in this study will allow the protein extended time and space to unfold, whereas in spread films, with the spreading method adopted in this study (*11*, *23*), the protein is forced into an interfacial space with little time or area to unfold. Another explanation would be the degree of packing of the interface; after successive compressions, at low surface coverage, the adsorbed film is likely to minimize energy and adopt a greater packing density than a spread film which is created more quickly, and is hence less likely to adopt the lowest energy structure. Thus, the structures of the films formed in the two different ways must be different, at least for adsorption from low bulk protein concentrations.

The surface pressure at the transition between structures I and II of an adsorbed β-casein film ($\pi_t^a \approx 12$ mN/m) is higher than that for a spread monolayer ($\pi_t^s \approx 10$ mN/m) (*23*). However, the transition between these structures is not as evident in the π−*A* isotherm for β-casein adsorbed films, as compared with spread monolayers (**Figure 1B**). BAM images also prove that β-casein spread (*23*, *29*) and adsorbed (**Figure 2A**) films adopt a homogeneous morphology during the first compression of the film. However, after successive compressions β-casein adsorbed films present some aggregations (**Figures 2B** and **2C**), which were not observed for spread monolayers (*23*, *29*).

For β-casein adsorbed films the surface dilatational modulus (*E*) versus surface pressure plots showed an irregular shape (**Figure 3A**), as observed with the same protein spread at the air−water interface (*11*). The values of *E* for β-casein films with structure II, and especially the minimum *E* value at the collapse point, are lower for spread than for adsorbed β-casein films. The fact that the values of *E* of β-casein is higher for adsorbed than for spread films suggests that β-casein in adsorbed films is more condensed (as deduced from data shown in **Figure 1B** for the displacement of the π−*A* isotherm toward lower area). That is, the film becomes more rigid as the protein unfolds and develops more intermolecular interactions because the slow formation of the adsorbed film in this study will allow the protein extended time and space to unfold. Thus, we do not reject the possibility that for a more viscoelastic adsorbed β-casein film (**Figure 3A**) its structure is more condensed than that obtained directly by spreading (**Figure 1B**). Upon further increase of the surface pressure (at $\pi > \pi_e^{\beta-\text{casein}}$) the differences in *E* values between adsorbed and spread β-casein films disappear with the formation of protein multilayers (*23*). In contrast with spread β-casein monolayers, which show viscoelastic behavior that changes to elastic at higher surface pressures, adsorbed β-casein films show viscoelastic behavior at every surface pressure (**Figure 3B**). Finally, if the frequency dependence of surface dilatational properties may be associated with the effect of the rate of deformation on the structure of β-casein films, at short time scales (at $\omega > 50$ mHz) the relaxation mechanism is essentially the same for adsorbed and spread β-casein films (**Figure 4**).

Adsorbed and Spread β-Casein−Monoglyceride Mixed Films. The structural characteristics of adsorbed mixed films (**Figures 5** and **9**) are in agreement with those deduced for spread β-casein + monoglyceride mixed films (*29*). That is, at low surface pressures (at $\pi < \pi_e^{\beta-\text{casein}}$) both β-casein and monoglyceride coexist at the interface, but protein displacement by the monoglyceride from the air−water interface takes place at $\pi > \pi_e^{\beta-\text{casein}}$. However, the kinetic character of the re-adsorption of previously displaced β-casein in adsorbed mixed films (**Figures 5B** and **9B**) was not evident for spread mixed films (*29*). The topographical characteristic of the adsorbed (**Figures 6** and **10**) and spread mixed films (*29*) are essentially similar, except in the presence of both short fractures near the collapse point of the mixed film (**Figure 6F**) and folds or aggregations of collapsed β-casein (**Figures 6D** and **10B**), which were not observed in spread mixed films (*29*).

In **Figures 7** and **11** are included the effect of surface pressure on viscoelastic properties of β-casein−monopalmitin and β-casein−monoolein mixed films adsorbed and spread (*31*) at the air−water interface, respectively. At $\pi < \pi_e^{\beta-\text{casein}}$ the $E-\pi$ plot showed an irregular shape, as for a pure β-casein adsorbed film (**Figure 3A**). The value of *E* was a maximum at the surface pressure of the transition between structures I and II for a spread mixed monolayer, but it is not evident for an adsorbed mixed film. These data corroborate that at $\pi < \pi_e^{\beta-\text{casein}}$ β-casein and monoglyceride coexist in adsorbed mixed films at the air−water interface with practically the same viscoelastic properties (**Figures 7** and **11**). However, at the higher surface pressures the *E* values of adsorbed β-casein + monoglyceride mixed films are lower than those for spread mixed monolayers at the same surface pressures. These results corroborate the idea that β-casein in adsorbed mixed films presents a higher resistance for its displacement by monoglyceride from the interface as compared with spread mixed monolayers. These results also corroborate the idea that β-casein in adsorbed mixed films presents a higher resistance to its displacement by monoolein from the interface as compared with spread mixed monolayers because the evolution of *E* with π is different for β-casein−monopalmitin and β-casein−monoolein mixed films, as compared with that for a pure monoglyceride monolayer.

Conclusions. In this work a unique device that incorporates different interfacial techniques, such as Wilhelmy-type film balance, Brewster angle microscopy, and interfacial dilatational rheology has been used to analyze the static (structure, morphology, and interactions) and dynamic characteristics (surface

dilatational properties) of β-casein−monoglyceride mixed films adsorbed on the air−water interface. The structural and topographical characteristics of β-casein and monoglycerides (monopalmitin and monoolein) adsorbed mixed films depend on the interfacial composition and the surface pressure. At $\pi < \pi_e^{\beta-\text{casein}}$ a mixed film of monoglyceride and β-casein may exist. At $\pi > \pi_e^{\beta-\text{casein}}$, the mixed films were dominated by monoglyceride molecules. That is, at higher surface pressures, collapsed β-casein residues may be partially displaced from the interface by monoglycerides. However, β-casein displacement by monoglycerides is not quantitative at the monoglyceride concentrations studied in this work. The protein displacement by monoglyceride is higher for monopalmitin than for monoolein and for spread than for adsorbed films. From a rheological point of view, β-casein−monoglyceride adsorbed films have viscoelastic character. At $\pi < \pi_e^{\beta-\text{casein}}$ the surface dilatational characteristics of the mixed films were dominated by the presence of β-casein in the mixture. Even at the higher surface pressures (at $\pi > \pi_e^{\beta-\text{casein}}$) the small amounts of β-casein collapsed residues with a variable extension and a random distribution at the interface have a significant effect on the surface dilatational properties of the mixed films.

From the comparison between viscoelastic characteristics of adsorbed (this work) and spread (*31*) β-casein−monoglyceride mixed films it can be concluded that (i) *E* values of β-casein adsorbed and spread films are similar, but the elastic character is higher for spread films, especially at higher surface pressures; (ii) *E* values at $\pi < \pi_e^{\beta-\text{casein}}$ for adsorbed and spread mixed films are the same, but significant differences were observed at $\pi > \pi_e^{\beta-\text{casein}}$, with the higher *E* values for spread mixed films; (iii) the viscoelasticity is higher for adsorbed than for spread mixed films; and (iv) viscoelastic characteristics of the mixed films corroborate the idea that protein displacement for monoglycerides is higher for spread than for adsorbed mixed films, especially for the β-casein−monopalmitin system.

One concluded that knowledge of interfacial structure of adsorbed emulsifiers (proteins and lipids) on a micro(nano)-scale and the interfacial properties derived from this structure (i.e., the surface dilatational properties) will have an important role in innovations in food dispersion formulations (emulsions and foams). In fact, the correlation between a specific product property and the micro(nano)-structure (*property function*) can be obtained by the choice of suitable process conditions (*process function*), such as surface pressure or surface density, surface composition, and film-forming formation (spreading, adsorption, or both). Thus, *product engineering* (or *formulation engineering*), which is concerned with physical or physicochemical principles, may improve quality and performance of products with adding value by the adequate correlation between property function and process function (*33*, *34*). We have observed recently that the thermodynamic and dynamic characteristics of adsorbed protein films have a significant role in the formation and stability of food model foam and emulsion formulated with this protein (*35*). However, the implications of nanoscience in product engineering of food dispersions formulated by these emulsifiers require further research (*36*).

ACKNOWLEDGMENT

The comments and suggestions raised by the referees are acknowledged.

LITERATURE CITED

(1) Dickinson, E. *An Introduction to Food Colloids*; Oxford University Press: Oxford, UK, 1992.

(2) Dickinson, E. Milk protein interfacial layers and the relationship to emulsion stability and rheology. *Colloids Surf., B* **2001**, *20*, 197−210.

(3) Bos, M. A.; van Vliet, T. Interfacial rheological properties of adsorbed protein layers and surfactants: a review. *Adv. Colloids Interface Sci.* **2001**, *91*, 437−471.

(4) Bos, M.; Nylander, T.; Arnebrant, T.; Clark, D. C. In *Food Emulsifiers and their Applications*; Hasenhuette, G. L., Hartel, R. W., Eds.; Chapman and Hall: New York, 1997; p 95.

(5) Wilde, P. J. Interfaces: their role in foam and emulsion behaviour. *Curr. Opin. Colloid Interface Sci.* **2000**, *5*, 176−181.

(6) Walstra, P. *Physical Chemistry of foods*; Marcel Dekker: New York, 2003.

(7) Wilde, P. J.; Mackie, A. R.; Husband, F.; Gunning, P.; Morris, V. Proteins and emulsifiers at liquid interfaces. *Adv. Colloid Interface Sci.* **2004**, *108−109*, 63−71.

(8) Rodríguez Patino, J. M.; Rodríguez Niño, M. R.; Carrera, C. Protein-emulsifier interactions at the air−water interface. *Curr. Opinion Colloid Interface Sci.* **2003,** *8*, 387−395.

(9) Pugnaloni, L. A.; Dickinson, E.; Ettelaie, R.; Mackie, A. R.; Wilde, P. J. Competitive adsorption of proteins and low-molecular-weight surfactants: computer simulation and microscopic imaging. *Adv. Colloid Interface Sci.* **2004**, *107*, 27−49.

(10) Rodríguez Patino, J. M.; Carrera, C.; Rodríguez Niño, M. R.; Cejudo, M. Structural-dilatational characteristics relationships of monoglyceride monolayers at the air−water interface. *Langmuir* **2001**, *17*, 4003−4013.

(11) Rodríguez Patino, J. M.; Carrera, C.; Rodríguez Niño, M. R.; Cejudo, M. Structural and dynamic properties of milk proteins at the air−water interface. *J. Colloid Interface Sci.* **2001**, *242*, 141−151.

(12) Murray, B. S.; Dickinson, E. Interfacial rheology and the dynamic properties of adsorbed films of food proteins and surfactants. *Food Sci. Technol. Inst.* **1996,** *2*, 131−145.

(13) Murray, B. S. In *Proteins at Liquid Interfaces*, Möbius, D., Miller, R., Eds.; Elsevier: Amsterdam, 1998; p 179.

(14) Murray, B. S. Interfacial rheology of food emulsifiers and proteins. *Curr. Opin. Colloid Interface Sci.* **2002**, *7*, 426−461.

(15) Lucassen-Reynders, E. H.; Benjamins, J. In *Food Emulsions and Foams: Interfaces, Interactions and Stability*; Dickinson, E., Rodríguez Patino, J. M., Eds.; Royal Society of Chemistry: Cambridge, 1999; p 195.

(16) Benjamins, J.; Lucassen-Reynders, E. H. In *Proteins at Liquid Interfaces*; Möbius, D., Miller, R., Eds.; Elsevier: Amsterdam, 1998; p 341.

(17) Rodríguez Patino, J. M.; Cejudo, M. Structural and topographical characteristics of adsorbed WPI and monoglyceride mixed monolayers at the air−water interface. *Langmuir* **2004**, *20*, 4515−4522.

(18) Fernández, M. C.; Sánchez, C. C.; Rodríguez Niño, M. R.; Rodríguez Patino, J. M. The effect of monoglycerides on structural and topographical characteristics of adsorbed β-casein films at the air−water interface. *Biomacromolecules* **2006**, *7*, 507−514.

(19) Rodríguez Niño, M. R.; Rodríguez Patino, J. M. Effect of the aqueous phase composition on the adsorption of bovine serum albumin to the air−water interface. *Ind. Eng. Chem. Res.* **2002**, *41*, 1489−1495.

(20) Rodríguez Niño, M. R.; Carrera, C.; Pizones, V.; Rodríguez Patino, J. M. Milk and soy protein films at the air−water interface. *Food Hydrocolloids* **2005**, *19*, 417−428.

(21) Rodríguez Niño, M. R.; Carrera, C.; Cejudo, M.; Rodríguez Patino, J. M. Protein and lipid adsorbed and spread films at the air−water interface at the equilibrium. *J. Am. Oil Chem. Soc.* **2001**, *78*, 873−879.

(22) Rodríguez Patino, J. M.; Carrera, C.; Rodríguez Niño, M. R. Morphological and structural characteristics of monoglyceride monolayers at the air−water interface observed by Brewster angle microscopy. *Langmuir* **1999**, *15*, 2484−2492.

(23) Rodríguez Patino, J. M.; Carrera, C.; Rodríguez Niño, M. R. Structural and morphological characteristics of β-casein monolayers at the air−water interface. *Food Hydrocolloids* **1999**, *13*, 401−408.
(24) Murray, B. S.; Faergemand, M.; Trotereau, M.; Ventura, A. In *Food Emulsions and Foams: Interfaces, Interactions and Stability*; Dickinson, E., Rodríguez Patino, J. M., Eds.; Royal Society of Chemistry: Cambridge, UK, 1999; p 223.
(25) Graham, D. E.; Phillips, M. C. Proteins at liquid interfaces. III. Molecular structures of adsorbed films. *J. Colloid Interface Sci.* **1979**, *70*, 427−439.
(26) Petkov, J. T.; Gurkov, T. D.; Campbell, B. E.; Borwankar, R. P. Dilatational and Shear Elasticity of Gel-like Protein Layers on Air/Water Interface. *Langmuir* **2000,** *16***,** 3703−3711.
(27) Serrien, G.; Geeraerts, G.; Ghosh, L.; Joos, P. Dynamic surface properties of adsorbed protein solutions: BSA, casein and buttermilk. *Colloids Surf.* **1992**, *68*, 219−233.
(28) Dussaud, A.; Vignes-Adler, M. Surface properties of protein alcoholic solutions: II. Surface dilational rheology. *J. Colloid Interface Sci.* **1994**, *167*, 256−265.
(29) Rodríguez Patino, J. M.; Carrera, C.; Rodríguez Niño, M. R. Analysis of β-casein-monopalmitin mixed films at the air−water interface. *J. Agric. Food Chem*. **1999**, *47*, 4998−5008.
(30) Li, J. B.; Krägel, J.; Makievski, A. V.; Fainermann, V. B.; Miller, R.; Möhwald, H. A study of mixed phospholipid/β-casein monolayers at the water/air surface. *Colloids Surf., A* **1998**, *142*, 355−360.
(31) Rodríguez Patino, J. M.; Rodríguez Niño, M. R.; Carrera, C. Structure, miscibility, and rheological characteristics of β-casein-monoglyceride mixed films at the air−water interface. *J. Agric. Food Chem*. **2004**, *51*, 112−119.
(32) Mackie, A. R.; Gunning, P. A.; Ridout, M. J.; Wilde, P. J.; Rodríguez Patino, J. M. In situ measurement of the displacement of protein films from the air/water interface by surfactant. *Biomacromolecules* **2001**, *2*, 1001−1006.
(33) Schubert, H.; Ax, K.; Behrend, O. Product engineering of dispersed systems. *Trends Food Sci. Technol.* **2003**, *14*, 9−16.
(34) He, L.; Dexter, A. F.; Middelberg, A. P. J. Biomolecular engineering at interfaces. *Chem. Eng. Sci*. **2006**, *61*, 689−1003.
(35) Carrera, S.; Rodríguez Patino, J. M. Interfacial, foaming and emulsifying characteristics of sodium caseinate as influenced by protein concentration in solution. *Food Hydrocolloids* **2005**, *19*, 407−416.
(36) Rodríguez Patino, J. M.; Lucero, A.; Rodríguez Niño, M. R.; Mackie, A. R.; Gunning, P.; Morris, V. J. Some implications of the nanoscience in food dispersion formulations containing phospholipids as emulsifiers. *Food Chem*. **2006**, in press.
(37) Birdi, K. S. *Lipid and Biopolymers Monolayers at Liquid Interfaces*; Plenum Press: New York, 1989.
(38) Rosenholm, J. B.; Ihalainem, P.; Peltonen, J. Thermodynamic characterization of Langmuir monolayers of thiolipids. A conceptual analysis. *Colloids Surf., A* **2003**, *228*, 119−130.

Received for review December 15, 2005. Revised manuscript received March 20, 2006. Accepted March 23, 2006. This research was supported by CICYT through Grant AGL2004-1306/ALI.

JF053142R